

The influence of heat treatment on the microstructural, mechanical and corrosion behaviour of cold sprayed SS 316L coatings

G. Sundararajan · P. Sudharshan Phani ·
A. Jyothirmayi · Ravi C. Gundakaram

Received: 4 June 2008 / Accepted: 15 December 2008 / Published online: 22 January 2009
© Springer Science+Business Media, LLC 2009

Abstract The present study evaluates the response of cold sprayed SS 316L coatings on mild steel substrate to aqueous corrosion in a 0.1 N HNO₃ solution as determined using polarization tests. The corrosion behaviour of the SS 316L coating was studied not only in the as-coated condition, but also after heat treatment at 400, 800 and 1,100 °C. Heat treatment reduced the porosity, improved inter-splat bonding, increased the elastic modulus and more importantly increased the corrosion resistance of the cold sprayed SS 316L coating.

Introduction

Cold gas dynamic spraying or cold spray is a powerful thermal spraying technique used to deposit a variety of materials [1–5]. The technique involves acceleration of powder particles typically in the size range 10–50 microns using a de Laval nozzle to velocities of the order of 600–1,000 m/s and subsequently coating formation upon impact on to a suitably prepared substrate [2]. The process details have been elaborated elsewhere [3, 4]. Unlike conventional thermal spraying processes, the cold spray process does not heat the powder particles significantly and thus provides an excellent means to produce coatings with low oxide

content and low thermal stresses [4, 5]. Corrosion protection and repair of offshore structures is a challenging task and cold spray technique offers an attractive opportunity to resolve these issues as there is a possibility of depositing protective coatings at high deposition rates and over large areas onsite using a portable cold spray unit.

Prior studies on stainless steel coatings using cold spray are very limited. Li et al. [6] studied the effect of particle velocity for SS 316L powder using cold spray and showed the possibility of obtaining dense SS 316L coatings using this technique. Other studies [7, 8] only deal with the deposition characteristics of stainless steel coatings but do not provide any data on corrosion behaviour.

Accordingly, the present study aims to comprehensively evaluate the aqueous corrosion (henceforth referred to as corrosion) behaviour of cold sprayed SS 316L coatings in the as-coated and heat-treated conditions. The influence of heat treatment of the cold sprayed SS 316L coating on corrosion behaviour has been included in the present study since numerous studies on heat treatment of a variety of metallic cold sprayed coatings [9–14] indicate enhancement of coating properties and performance upon heat treatment due to improved inter-splat bonding within the coating. Finally, to benchmark the corrosion behaviour of cold sprayed SS 316L, the corrosion behaviour of bulk SS 316L was also evaluated.

Experimental procedure

Materials and coating deposition

Stainless steel coatings were deposited using the in-house facility for cold spraying. A De Laval nozzle with a rectangular exit was used for the present study. Compressed air

G. Sundararajan (✉) · P. Sudharshan Phani · A. Jyothirmayi ·
R. C. Gundakaram
International Advanced Research Centre for Powder Metallurgy
and New Materials (ARCI), Balapur (P.O.),
Hyderabad 500 005, India
e-mail: gsundar@arci.res.in

P. Sudharshan Phani
e-mail: sphani@yahoo.com

was used as the process gas as well as the powder carrier gas. Commercially available SS 316L stainless steel powder (FE-101, Praxair, USA) was used as the feedstock. The average powder particle size, as reported by the manufacturer, was -45 to $+15$ μm . Grit blasted mild steel was used as the substrate. These specimens were subjected to thorough ultrasonic cleaning prior to coating deposition for better adhesion. Preliminary trials were carried out to optimize the coating parameters. Coatings were then deposited at the optimum conditions, i.e. a stagnation temperature of 475 $^{\circ}\text{C}$ and a stagnation pressure of 2.0 MPa. A constant stand off distance of 15 mm was maintained for all the coatings.

Heat treatment

The stainless steel coatings were subjected to heat treatment at three different temperatures— 400 $^{\circ}\text{C}$, 800 $^{\circ}\text{C}$ and 1100 $^{\circ}\text{C}$ to study the effect of heat treatment on the corrosion response. The treatments were carried out in air and the specimens were held at the treatment temperature for 1 h followed by cooling in air.

Microstructural characterization

A field emission-scanning electron microscope (Hitachi—S4300SE/N, Japan) and a scanning electron microscope (Hitachi—S3400 N, Japan) were used for carrying out microscopic examination of the morphology of the powder and microstructure of the coatings. EBSD attachment to SEM was used to estimate the twin volume fraction especially in heat-treated cold sprayed SS 316L coatings. Coated specimens and heat-treated specimens were sectioned and the sectioned face was mounted using bakelite for metallographic polishing. Coating porosity was measured using an Image Analyzer system (Image Pro Plus, Media Cyber Netics, USA) attached to an optical microscope. An aqueous solution of 15 mL HCl, 5 mL HNO_3 and 100 mL H_2O was used for etching the samples. Coating hardness was measured using a Vickers microhardness tester (Leitz-112473, Germany) at a load of 100 g. At least 10 measurements were taken in a staggered manner on the coating cross section and the readings were within $\pm 6\%$ of the reported mean value. Elastic modulus was measured using a nanoindenter utilizing the technique described by Oliver and Pharr [15].

Evaluation of corrosion resistance

The corrosion behaviour of cold sprayed SS 316L coating was evaluated by means of polarization tests carried out using a Solartron 1260 Impedance/Gain Phase analyzer with a Solartron 1287 Electrochemical Interface. As-coated

and heat-treated stainless steel coatings and bulk SS 316L were exposed to 0.1 N HNO_3 solution. The 3-electrode potentiostatic mode was applied with a saturated calomel reference electrode (SCE). Platinum electrode was used as a counter electrode. Polarization tests were carried out at a scan rate of 1 mV/s. With this experimental set up data were collected at different time intervals and the data were analysed using the Corrware and Corrview software. Polarization tests were carried out twice on selected samples and it was observed that E_{corr} values were well within 1% of each other.

In the present set of polarization experiments, as will be shown later, the samples passivated immediately on immersion and the passivity was stable with continued immersion. In such a case, it is inappropriate to use anodic Tafel constants for determining the corrosion rate. Therefore, it was decided to use the polarization resistance (R_p) as the measure of corrosion resistance. The linear polarization technique takes advantage of the fact that within ± 20 mV of the corrosion potential, the plot of applied potential versus measured current is often linear. The slope of this linear plot (i.e. $\Delta E/\Delta i_{\text{app}}$) equals R_p (units: Ω/cm^2).

Results and discussion

Coating microstructure

Figure 1 shows the typical cross-sectional view of the as-coated stainless steel coating on mild steel substrate as well as the specimens heat-treated at 400 $^{\circ}\text{C}$, 800 $^{\circ}\text{C}$ and 1100 $^{\circ}\text{C}$. These micrographs clearly indicate the highly dense nature of the coatings. Excellent bonding between the coating and the substrate is also evident from these micrographs.

A higher magnification sectional view of the stainless steel coatings (after etching) is presented in Fig. 2. In the as-coated condition, the presence of numerous inter-splat voids (identified by letter A in Fig. 2) and also the weakly bonded inter-splat boundaries (marked by letter B in Fig. 2) is evident. With increasing heat treatment temperature, the bonding between the splats improves continuously as evident from the decrease in the number of weakly bonded inter-splat boundaries when Fig. 2b, c and d are compared.

The influence of heat treatment on the porosity of the coating, as measured using the image analyser system, is presented in Table 1. It is clear that the porosity of the coating decreases substantially after heat treatment at 800 $^{\circ}\text{C}$ and $1,100$ $^{\circ}\text{C}$. These data are also broadly consistent with the SEM micrographs of the coatings presented in Fig. 2. However, it also appears that the porosity levels seen in Fig. 2 are more than 1% while the

Fig. 1 SEM micrographs (BSE mode) of coating cross section in **a** as coated, **b** heat-treated—400 °C, **c** heat-treated—800 °C, **d** heat-treated—1,100 °C

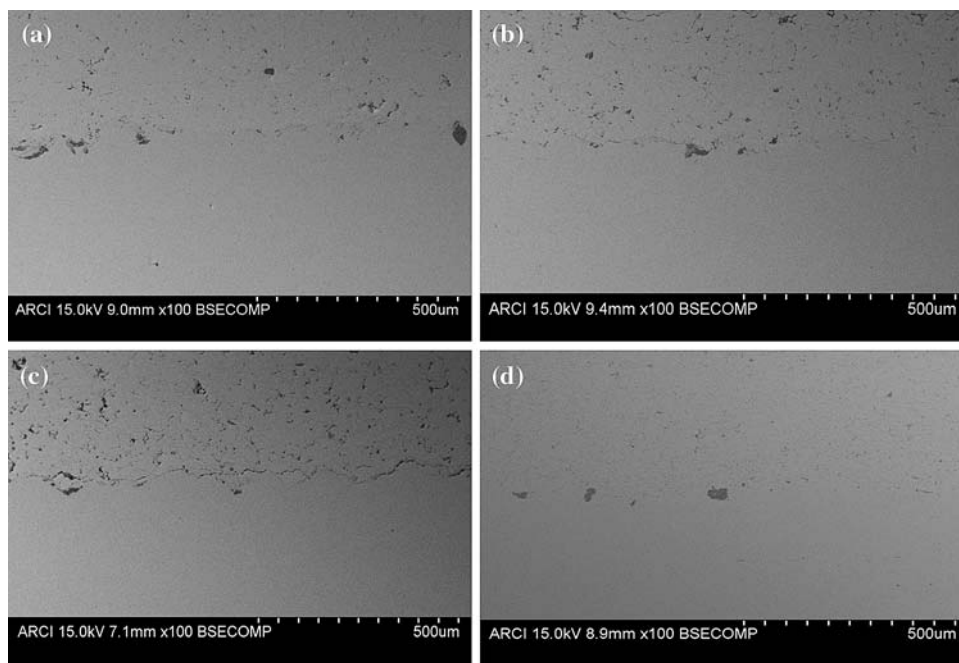


Fig. 2 SEM micrographs of cold spray coatings after etching in the **a** as coated, **b** heat-treated—400 °C, **c** heat-treated—800 °C, **d** heat-treated—1,100 °C. Symbols A and B are explained in the text

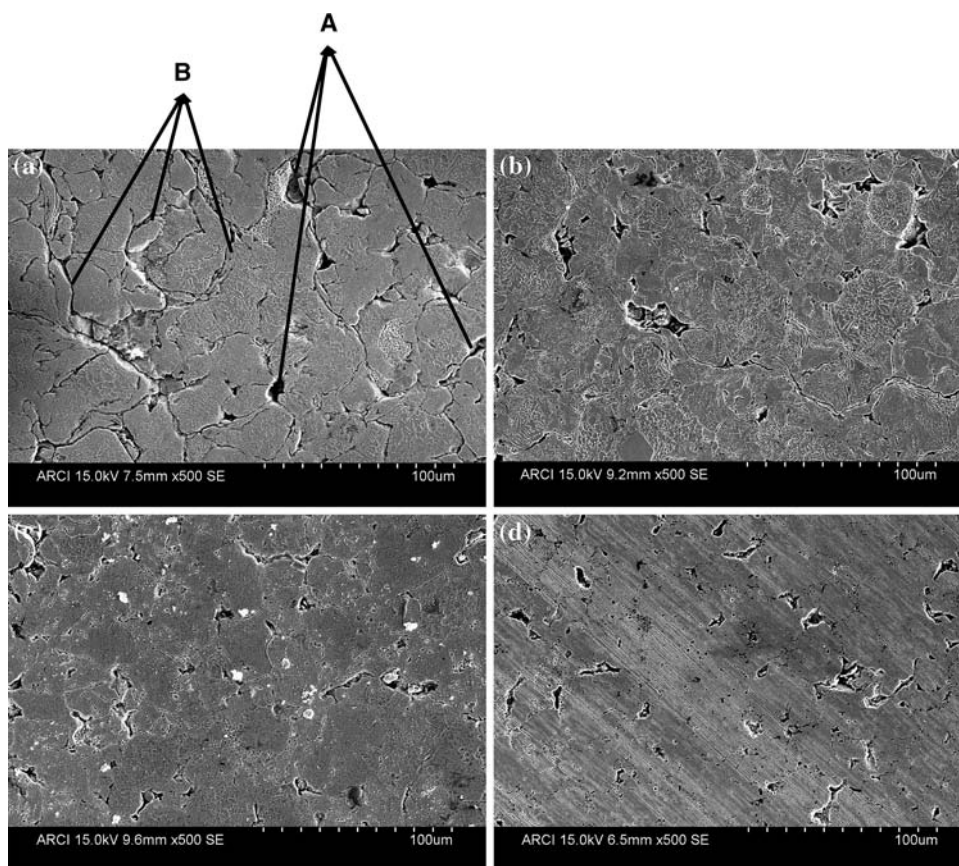


image analysis gives porosity levels lower than 1%. This discrepancy is most probably due to the fact that the image analysis was carried out using an optical microscope at a lower magnification of 200 \times (as opposed to SEM images at 500 \times in Fig. 2) and also because porosity

analysis was done on unetched surfaces, while SEM images (in Fig. 2) represent severely etched surfaces (required to reveal the inter-splat boundaries) and it is likely that severe etching opened out the pores and inter-splat cracks.

Table 1 The influence of heat treatment on the hardness, elastic modulus, fraction of the twin boundaries and porosity of the SS 316L cold sprayed coatings

Sl. No.	Heat treatment temp. (°C)	Hardness (GPa)	Elastic modulus (GPa)	Normalised elastic modulus ^a	Fraction of twin boundaries	Porosity %
1	As coated	2.924	98.43	0.51	0.015	0.80
2	400	2.604	104.89	0.54	0.023	0.76
3	800	2.202	161.80	0.83	0.212	0.36
4	1100	2.114	164.42	0.85	0.214	0.20

^a Normalised elastic modulus = Elastic modulus of the SS 316L coating/elastic modulus of the bulk SS 316L (193 GPa)

Using the EBSD attachment to the SEM, the presence of twins (essentially annealing twins) in the cold sprayed SS 316L coatings as a function of heat treatment temperature was examined. For example, Fig. 3b provides the EBSD image of the coating over an area corresponding to that depicted in Fig. 3a, for SS 316L coating heat-treated at 1,100 °C. The presence of annealing twins and the development of clear grain boundaries due to recrystallization are evident. In the case of coatings in the as-coated and heat-treated conditions (at 400 °C), the presence of annealing twins were negligible and the grain boundaries were not at all well defined. EBSD analysis also gave a quantitative analysis of the fraction of grain boundaries corresponding to twins as a function of heat treatment temperature as illustrated in Table 1. Thus, only the coatings heat-treated at 800 °C and 1,100 °C had a substantial fraction of twins, i.e. around 20%.

Mechanical behaviour of coating

The hardness of the cold sprayed SS 316L coating decreases continuously with increasing heat treatment temperature as shown in Table 1. The above decrease in hardness is largely due to the elimination of cold work effects and subsequent recrystallization with increasing heat treatment temperature.

The variation of elastic modulus of the SS 316L coating with heat treatment temperature is also presented in Table 1. In the same Table, the ratio of the elastic modulus of the coating to that of bulk SS 316L is also indicated (Elastic modulus of bulk SS 316L = 193 GPa). In the as-coated condition and also after heat treatment at 400 °C, the elastic modulus of the coating is very low (≈ 100 GPa) and is about 50% of the elastic modulus value of bulk SS 316L. Such a low elastic modulus value is consistent with the presence of extensive separated inter-splat boundaries as can be observed in Fig. 2a and b. Such separated inter-splat boundaries can be treated as cracks and presence of numerous cracks can cause the elastic modulus to decrease significantly as demonstrated already by number of investigators [16–18]. However, consistent with the fact that

heat treatment of the coating at 800 °C and 1,100 °C reduces the number density of separated inter-splat boundaries (see Fig. 2c, d), the elastic modulus of the coating increases substantially to almost 85% of the bulk value as depicted in Table 1. Even after heat treatment at 1,100 °C, the elastic modulus is still lower than the bulk value largely due to the presence of isolated voids (Figs. 2d, 3).

Corrosion behaviour of coatings

Polarization tests were carried out on the as-coated and heat-treated SS 316L specimens after 1 h and 24 h of immersion in 0.1 N HNO₃ solution. Bulk SS 316L and mild steel specimens were also subjected to polarization tests in order to provide reference values. Cold spray coating does have porosity and it is possible that the electrolyte can penetrate the coating through such pores and attack the substrate if the immersion time is sufficiently large. Therefore, it was decided to carry out polarization tests after 1 h and 24 h immersion.

Figure 4 presents the polarization curve (E vs. $\log i$) in respect of as-coated and heat-treated cold sprayed SS 316L coatings and bulk SS 316L after immersion in 0.1 N HNO₃ solution for 1 h (Fig. 4a) and 24 h (Fig. 4b), respectively. The polarization curve for mild steel after immersion for 1 h is also provided in Fig. 4a. Figure 4a clearly illustrates the fact that SS 316L, irrespective of whether it is in bulk form or in the form of coating, is clearly superior to mild steel in terms of corrosion resistance. To evaluate and compare the corrosion resistance of bulk and coated SS 316L, the polarization resistance (R_p) was used as the measure and R_p was determined using the procedure described in section “Evaluation of corrosion resistance”.

Figures 5 and 6 present the variation of corrosion potential (E_{corr}) and polarization resistance (R_p) of cold sprayed SS 316L coatings (after 1 h immersion) as a function of heat treatment temperature (represented by filled circles). Similar data from the samples immersed in 0.1 HNO₃ solution for 24 h are also presented in Figs. 5 and 6 as unfilled circles.

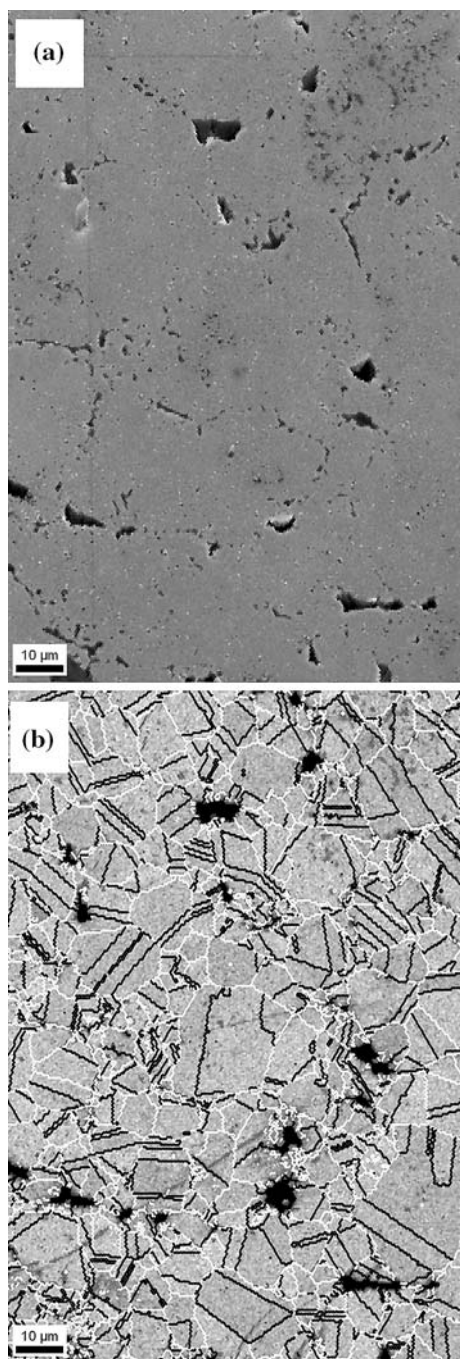


Fig. 3 SEM micrograph (a) and image quality map (b) of the same area, with the latter delineating the twin boundaries, obtained on cold sprayed stainless steel coatings heat-treated at 1,100 °C

It is clear from Figs. 5 and 6 that the cold sprayed SS 316L coatings in the as-coated condition exhibits a corrosion potential which is more negative (−0.25 V) than bulk SS 316L (−0.19 V) but substantially nobler than the mild steel (−0.54 V). The corrosion resistance (i.e. R_p) of as-coated SS 316L (153.0 Ω/cm^2) is nearly 20 times lower than that of bulk SS 316L (3095.0 Ω/cm^2) after 1 h

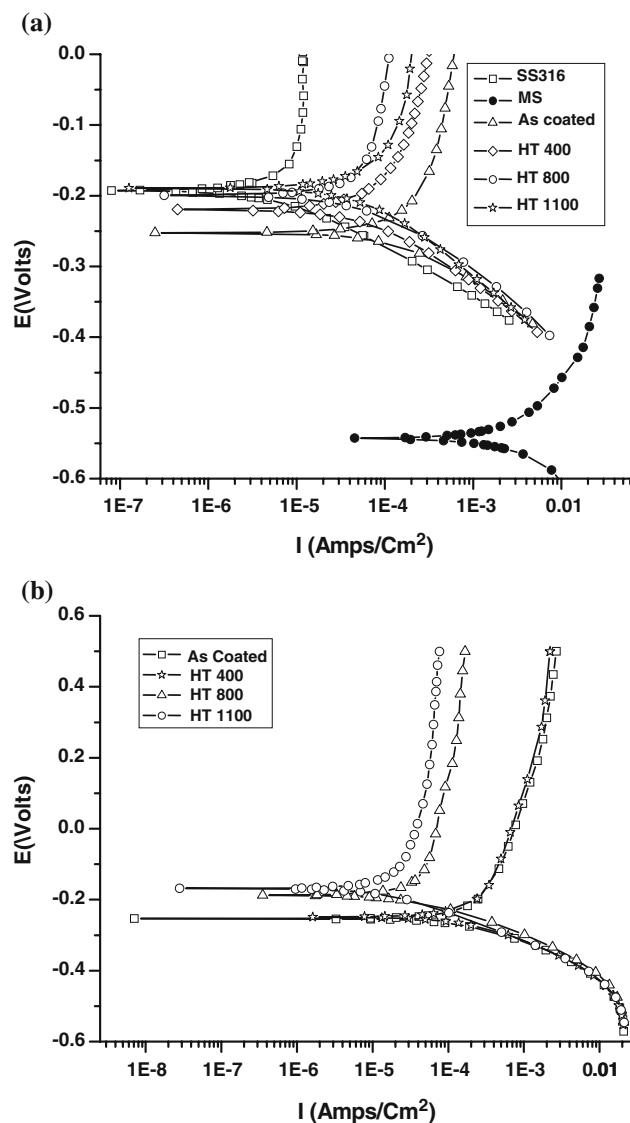


Fig. 4 Polarization behaviour of cold sprayed stainless steel coatings after (a) 1 h exposure (b) 24 h exposure in 0.1 N HNO₃ solution

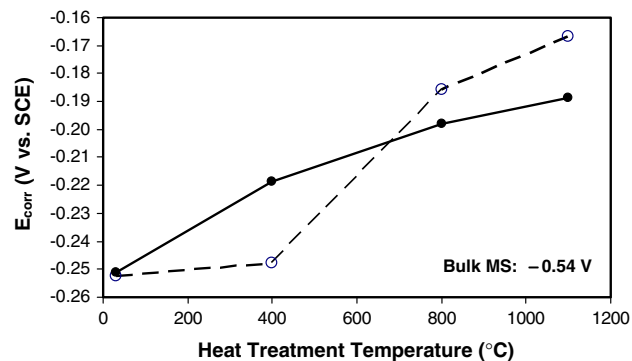


Fig. 5 The variation of corrosion potential with heat treatment temperature after 1 h (filled circles) and 24 h (unfilled circles) of immersion in 0.1 N HNO₃ solution

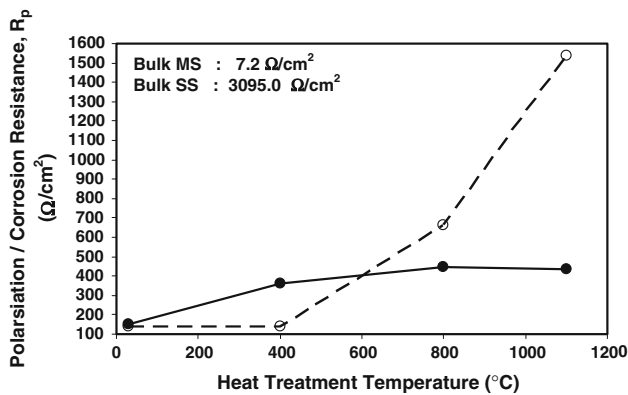


Fig. 6 The variation of polarization/corrosion resistance with heat treatment temperature after 1 h (filled circles) and 24 h (unfilled circles) of immersion in 0.1 N HNO_3 solution

immersion. In contrast, after 24 h immersion in HNO_3 solution, the as-coated SS 316L exhibits a corrosion resistance 40 times lower than that of bulk SS 316L. However, when compared to bare mild steel ($E_{\text{corr}} = -0.54$ V and $R_p = 7.2 \Omega/\text{cm}^2$), a cold sprayed SS 316L coating on mild steel results in a corrosion potential that is substantially nobler ($E_{\text{corr}} = -0.25$ V) and a corrosion resistance (i.e., R_p) that is nearly 20 times higher. Thus, even in the as-coated condition, cold sprayed SS 316L coating does provide corrosion protection to the mild steel substrate.

Heat treatment of the cold sprayed SS 316L coating, especially at temperatures of 800 °C and 1,100 °C, does improve the corrosion behaviour as can be observed from Figs. 5 and 6. For example, cold sprayed SS 316L coating heat-treated at 1,100 °C exhibits a corrosion resistance (R_p) only a factor of 4 lower than that of bulk SS 316L after 24 h immersion in HNO_3 solution. However, after 1 h immersion, the corrosion resistance (i.e., R_p) of the coating heat-treated at 800 °C and 1,100 °C is lower by a factor of 7. In the case of bulk SS 316L, the corrosion resistance after 24 h immersion is lower than after 1 h immersion. In the case of cold sprayed SS 316L, such a behaviour is replicated only after heat treatment at 1,100 °C and 800 °C. Thus, it can be concluded that the cold sprayed SS 316L exhibits near bulk behaviour only after such high temperature treatment quite consistent with the microstructural features provided in Fig. 2.

Discussion

The main outcome of the present study is that cold-sprayed SS 316L coatings in the as coated condition, exhibit corrosion resistance substantially superior to the mild steel substrate but inferior to that of bulk SS 316L.

The present study also demonstrates that heat treatment of the cold sprayed coating does improve its microstructure and corrosion properties and in particular, heat treatment at 1,100 °C for 1 h, results in the best corrosion resistance.

The improvement in corrosion resistance with increasing heat treatment temperature, in our opinion, is the result of improved microstructure characterized by fewer weakly bonded/unbonded inter-splat boundaries as a result of heat treatment (see Fig. 2). It is unlikely that presence of annealing twins (after heat treatment at 800 °C and 1,100 °C) in the cold sprayed SS 316L coating has any influence on the corrosion behaviour. As long as weakly or unbonded inter-splat boundaries are present in sufficient numbers in the coating, they provide a least resistance path for the electrolyte to penetrate the coating, reach the coating–substrate interface, and thereby cause the corrosion of the mild steel substrate underneath. Preliminary results from EIS studies (Sudharshan Phani et al. 2007, Unpublished research) not presented here, do confirm the above postulate. In particular, cold sprayed SS 316L coating in the as-coated and heat-treated at 400 °C resulted in Bode plots with two time constants which merged into a semicircle with one time constant in the case of coatings heat-treated at 800 °C and 1,100 °C.

Conclusions

1. The cold sprayed SS 316L coating, in the as-coated condition, exhibits a microstructure characterized by weakly/unbonded inter-splat boundaries, high porosity and elastic modulus around 50% of the value expected for dense SS 316L.
2. With increasing heat treatment temperature, the density of weakly/unbonded inter-splat boundaries and porosity decrease with a corresponding increase in elastic modulus.
3. The cold sprayed SS 316L coating, in the as-coated condition, exhibits a corrosion rate 20 times lower than mild steel substrate but 20–40 times higher than bulk SS 316L.
4. With increasing heat treatment temperature, the corrosion rate of cold sprayed SS 316L coating decreases and ultimately reaches a value quite close to that of bulk SS 316L after heat treatment at 1,100 °C.

Acknowledgements The authors wish to thank Director, International Advanced Research Centre for Powder Metallurgy and New Materials (ARCI) for granting permission to publish this paper. We also express our gratitude to the reviewers whose comments have certainly improved the quality of the paper.

References

1. Karthikeyan J, Kay CM (2003) In: Marple BR, Moreau C (eds) Thermal spray: advancing the science and applying the technology. ASM International, Orlando, p 117
2. Alkimov AP, Papyrin AN, Kosarev VF, Nesterovich NJ, Shuspanov MM (1994) US patent 5,302,414
3. Dykhuizen RC, Smith MF, Gilmore DL et al (1999) *J Thermal Spray Technol* 8:559
4. Kreye H, Stoltenhoff T (2000) In: Berndt CC (ed) Thermal spray: surface engineering via applied research. ASM International, Montreal, p 419
5. Stoltenhoff T, Kreye H, Richter HJ (2002) *J Thermal Spray Technol* 11:542
6. Li W-Y, Liao H, Douchy G et al (2007) *Mater Des* 28:2129
7. Voyer J, Stoltenhoff T, Kreye H (2003) In: Marple BR, Moreau C (eds) Thermal spray: advancing the science and applying the technology. ASM International, Orlando, p 71
8. Schmidt T, Gartner F, Assadi H et al (2006) *Acta Mater* 54:729
9. Sudharshan Phani P, Vishnukanthan V, Sundararajan G (2007) *Acta Mater* 55:4741
10. Sudharshan Phani P, Srinivasa Rao D, Joshi SV, Sundararajan G (2007) *J Thermal Spray Technol* 16:425
11. Li W-Y, Li C-J, Liao H (2006) *J Thermal Spray Technol* 15:206
12. Borchers C, Gartner F, Stoltenhoff T, Kreye H (2005) *Acta Mater* 53:2991
13. Gartner F, Stoltenhoff T, Voyer J et al (2006) *Surf Coat Technol* 200:6770
14. Stoltenhoff T, Borchers C, Gartner F, Kreye H (2006) *Surf Coat Technol* 200:4947
15. Oliver WC, Pharr GM (1992) *J Mater Res* 7:1564
16. Thompson JA, Clyne TW (2001) *Acta Mater* 49:1565
17. Nakamura T, Qian G, Berndt CC (2000) *J Am Ceram Soc* 83:578
18. Luo J, Stevens R (1999) *Ceram Inter* 25:281